

# Longitudinal distribution of nitrate $\delta^{15}\text{N}$ and $\delta^{18}\text{O}$ in two contrasting tropical rivers: implications for instream nitrogen cycling

Toshihiro Miyajima · Chikage Yoshimizu ·  
Yoshie Tsuboi · Yoshiyuki Tanaka · Ichiro Tayasu ·  
Toshi Nagata · Isao Koike

Received: 11 July 2008 / Accepted: 25 May 2009 / Published online: 18 June 2009  
© Springer Science+Business Media B.V. 2009

**Abstract** The longitudinal variations in the nitrogen ( $\delta^{15}\text{N}$ ) and oxygen ( $\delta^{18}\text{O}$ ) isotopic compositions of nitrate ( $\text{NO}_3^-$ ), the carbon isotopic composition ( $\delta^{13}\text{C}$ ) of dissolved inorganic carbon (DIC) and the  $\delta^{13}\text{C}$  and  $\delta^{15}\text{N}$  of particulate organic matter were determined in two Southeast Asian rivers contrasting in the watershed geology and land use to understand internal nitrogen cycling processes. The  $\delta^{15}\text{N}_{\text{NO}_3}$  became higher longitudinally in the freshwater reach of both rivers. The  $\delta^{18}\text{O}_{\text{NO}_3}$  also increased longitudinally in the river with a relatively steeper longitudinal gradient and a less cultivated watershed, while the  $\delta^{18}\text{O}_{\text{NO}_3}$  gradually decreased in the other river. A simple model for the  $\delta^{15}\text{N}_{\text{NO}_3}$  and the  $\delta^{18}\text{O}_{\text{NO}_3}$  that accounts for simultaneous input and removal of

$\text{NO}_3^-$  suggested that the dynamics of  $\text{NO}_3^-$  in the former river were controlled by the internal production by nitrification and the removal by denitrification, whereas that in the latter river was significantly affected by the anthropogenic  $\text{NO}_3^-$  loading in addition to the denitrification and/or assimilation. In the freshwater-brackish transition zone, heterotrophic activities in the river water were apparently elevated as indicated by minimal dissolved oxygen, minimal  $\delta^{13}\text{C}_{\text{DIC}}$  and maximal  $p\text{CO}_2$ . The  $\delta^{15}\text{N}$  of suspended particulate nitrogen (PN) varied in parallel to the  $\delta^{15}\text{N}_{\text{NO}_3}$  there, suggesting that the biochemical recycling processes (remineralization of PN coupled to nitrification, and assimilation of  $\text{NO}_3^-$ -N back to PN) played dominant roles in the instream nitrogen

T. Miyajima · Y. Tsuboi · Y. Tanaka ·  
T. Nagata · I. Koike  
Ocean Research Institute, The University of Tokyo,  
Nakano, Tokyo 164-8639, Japan

C. Yoshimizu · I. Tayasu · T. Nagata  
Center for Ecological Research, Kyoto University, Hirano,  
Otsu 520-2113, Japan

C. Yoshimizu  
Japan Science and Technology Agency, Kawaguchi,  
Saitama 332-0012, Japan

*Present Address:*  
Y. Tsuboi  
Kurume Laboratory, Chemicals Evaluation and Research  
Institute, Japan, Miyanoin, Kurume 839-0801, Japan

*Present Address:*  
Y. Tanaka  
International College of Arts and Sciences, Yokohama  
City University, Kanazawa, Yokohama 236-0027, Japan

*Present Address:*  
I. Koike  
University of the Ryukyus, Nishihara, Okinawa 903-0213,  
Japan

T. Miyajima (✉)  
Department of Chemical Oceanography, Ocean Research  
Institute, The University of Tokyo, Minamidai 1-15-1,  
Nakano, Tokyo 164-8639, Japan  
e-mail: miyajima@ori.u-tokyo.ac.jp

transformation. In the brackish zone of both rivers, the  $\delta^{15}\text{N}_{\text{NO}_3}$  displayed a declining trend while the  $\delta^{18}\text{O}_{\text{NO}_3}$  increased sharply. The redox cycling of  $\text{NO}_3^-/\text{NO}_2^-$  and/or deposition of atmospheric nitrogen oxides may have been the major controlling factor for the estuarine  $\delta^{15}\text{N}_{\text{NO}_3}$  and  $\delta^{18}\text{O}_{\text{NO}_3}$ , however, the exact mechanism behind the observed trends is currently unresolved.

**Keywords** Anthropogenic nitrogen loading · Denitrification · Estuary · Nitrate · Nitrification · Tropical river

## Introduction

Transport of terrestrial nitrogen through rivers and estuaries is one of the major links between terrestrial and marine nitrogen cycles and exerts a strong influence on the development, productivity and biodiversity of the coastal marine ecosystems. Since the tropical surface ocean is usually depleted of inorganic nutrients, especially dissolved inorganic nitrogen (DIN), river-borne nutrient input is the major external source of nitrogen and constrains the metabolic activities of tropical coastal communities. A moderate loading of DIN by river discharge would enhance both the productivity and the biodiversity of coastal ocean. However, increasing population, agricultural advancement and urbanization in coastal areas especially in Southeast Asian countries have resulted in increasing nitrogen loading from watersheds to rivers and significant nitrate pollution in lower-reach rivers, estuaries and groundwaters in recent years (Seitzinger and Kroeze 1998; Jennerjahn et al. 2004; Umezawa et al. 2008). Excess DIN loading by rivers and groundwaters to the coastal ocean causes the deterioration of coastal ecosystems, particularly benthos-dominated ones such as coral reefs and seagrass beds (Lapointe et al. 2004). It has been well recognized that, as external DIN loading increases, these benthic communities that are adapted to low-nutrient tropical oceans are gradually replaced by macroalga-dominated communities that are more adaptive to eutrophic waters, although the exact mechanism behind this replacement is still controversial (McCook et al. 2001). Eutrophication stimulates microalgal productivity, and the shading effect

by dense phytoplankton and epiphytic algal population restricts productivity of seagrasses and hermatypic corals (Lapointe and Clark 1992). In deeper bays and gulfs, the enhanced primary production as well as the increased organic loading by the terrestrial runoff accelerates the oxygen consumption in the stratified bottom waters and sometimes results in the formation of the hypoxia and the anoxia, often called “coastal dead zone” (Diaz and Rosenberg 2008). Elevated phytoplankton production also causes complex responses of ecosystems, such as the enhancement of larval survival of the coral-eating echinoderm *Acanthaster planci*, which in turn accelerates the decline of reef corals by its grazing activity (Bell 1992; Brodie et al. 2005). Therefore, control and regulation of terrestrial nitrogen loading by river and groundwater discharge is an urgent demand for the protection, restoration and effective management of tropical coastal natural resources.

Terrestrial nitrogen is transported by rivers and groundwaters principally in the form of nitrate ( $\text{NO}_3^-$ ). The concentration and the flux of  $\text{NO}_3^-$  in a given river or aquifer depend on hydrology, geology, vegetation and human land use in the watershed, and are specifically constrained by nitrogen influxes to the watershed through natural nitrogen fixation, atmospheric deposition and anthropogenic nitrogen loading, which have traditionally been estimated by load-factor calculations for potential point and non-point sources. However,  $\text{NO}_3^-$  is not simply externally loaded to and transported by river waters, but also continually turned over within the river channel by internal biogeochemical processes such as assimilation, remineralization, nitrification and denitrification (Mulholland 1992; Bernhardt et al. 2003; Sebilo et al. 2003). These processes are potentially of pivotal importance in determining the actual discharge rates of  $\text{NO}_3^-$  through rivers to coastal seas. To evaluate quantitatively the influences of these internal processes, simple monitoring of the  $\text{NO}_3^-$  concentration and the river discharge is not sufficient, but direct and extensive measurements of specific metabolic activities in river waters and riverbeds are required. However, such measurements are usually expensive, laborious and time-consuming. Consequently, reliable estimation has often been lacking especially for tropical rivers. The lack of such information has restricted the potential to accurately predict responses of river and coastal marine

environments to increasing human activities and global climate change, particularly in tropical regions.

During the last decade, the stable nitrogen ( $\delta^{15}\text{N}$ ) and oxygen ( $\delta^{18}\text{O}$ ) isotopic signatures of  $\text{NO}_3^-$  have increasingly been used for scaling internal biochemical processes responsible for  $\text{NO}_3^-$  turnover in rivers and groundwaters (Kendall et al. 2007). These signatures vary sensitively in response to the internal removal processes of  $\text{NO}_3^-$  such as assimilatory reduction by aquatic plants and bacteria and dissimilatory reduction including denitrification (Fig. 1). The degree of variation depends on specific processes. Furthermore, since  $\text{NO}_3^-$  of different origins often exhibits much different  $\delta^{15}\text{N}$  and  $\delta^{18}\text{O}$  signatures, these signatures of river-water  $\text{NO}_3^-$  can be used to trace the sources of  $\text{NO}_3^-$  and estimate the relative strength of each source (Fig. 1). Previously, the measurement of  $\delta^{15}\text{N}_{\text{NO}_3}$  and  $\delta^{18}\text{O}_{\text{NO}_3}$  required very laborious and time-consuming preparation processes and relatively large volume of samples. Particularly, the  $\delta^{18}\text{O}_{\text{NO}_3}$  measurement of saline water samples was virtually impossible. However, recent development of the denitrifier method by Sigman et al. (2001) and Casciotti et al. (2002) has enabled the determination of the  $\delta^{15}\text{N}$  and  $\delta^{18}\text{O}$  of  $\text{NO}_3^-$  in natural water samples including seawater simultaneously with sufficient accuracy and precision and with a high throughput. This method also requires relatively small amounts ( $\leq 10$  ml) of samples, which especially facilitates extensive monitoring and synoptic observation in distant survey sites such as tropical rivers. However, the combined use of  $\delta^{15}\text{N}_{\text{NO}_3}$  and  $\delta^{18}\text{O}_{\text{NO}_3}$  for the study of river nitrogen dynamics has been mostly confined to date within applications to temperate rivers (Sebilo et al. 2006; Kendall et al. 2007; Ruehl et al. 2007).

In the present study, the influences of internal turnover processes on the dynamics of  $\text{NO}_3^-$  in two tropical rivers was investigated by observing the longitudinal variations of  $\delta^{15}\text{N}_{\text{NO}_3}$  and  $\delta^{18}\text{O}_{\text{NO}_3}$  from the upper reach down to the estuary. A simple model that relates  $\delta^{15}\text{N}_{\text{NO}_3}$  and  $\delta^{18}\text{O}_{\text{NO}_3}$  to the turnover processes of  $\text{NO}_3^-$  was devised and used to infer the dominant removal processes and the major sources of  $\text{NO}_3^-$ . To compare the functioning of the instream metabolic processes in the nitrogen cycle to that in the carbon cycle, the longitudinal variations in the carbon isotope ratio ( $\delta^{13}\text{C}$ ) of dissolved inorganic carbon (DIC) and the  $\delta^{13}\text{C}$  and  $\delta^{15}\text{N}$  of suspended particulate organic matter were also investigated.

## Study sites

The survey took place in two rivers, the Khura River on 13 and 15 Dec. 2006 and the Trang River on 18 and 21 Dec. 2006, both draining peninsular Thailand to the Andaman Sea (Fig. 2). The river-path length from the most upstream sampling station to the river mouth station was 31.5 and 204 km for the Khura and Trang Rivers, respectively, and between these end points, additional 19 and 24 sampling points were set, respectively. The river mouth station of the Khura River was located at  $9^\circ 14.80'\text{N}$   $98^\circ 19.88'\text{E}$ , and that of the Trang River at  $7^\circ 13.54'\text{N}$   $99^\circ 24.51'\text{E}$ . The Khura River drains predominantly granitic basin, while the watershed geology of the Trang River is dominated by granite bedrocks in the upper reach and sedimentary rocks including limestone and calcareous shale in the middle to lower reach (Department of Mineral Resources of Thailand; [www.dmr.go.th/DMR\\_eng/](http://www.dmr.go.th/DMR_eng/)). Human population density of the Phangnga district that includes the Khura River watershed is 56 inhabitants  $\text{km}^{-2}$ , while that of the Trang River watershed is 146 inhabitants  $\text{km}^{-2}$ . December was just the onset of the dry season and the precipitation was low (ca. 60 and 110  $\text{mm month}^{-1}$  in the Phangnga and Trang districts, respectively). However, the river discharge was still high due to the precipitation during the preceding rainy season, especially in the Trang River where the rainy season ends somewhat later than around the Khura River.

Unfortunately, we have no hydrological data for these rivers during the study period. In the Trang River, water discharge had been monitored during 1966–1984 at a gauging station ca. 90 km upstream of the river mouth station. The average discharge rate in December of the most recent 5 years (1980–84) was  $98.5 \pm 65.8 \text{ m}^3 \text{ s}^{-1}$  (mean  $\pm$  SD; Vörösmarty et al. 1996), which was approximately 15 times higher than the discharge under the baseflow conditions in March (late dry season). The watershed area at this gauging station is ca. 1,800  $\text{km}^2$ , while the watershed area of the Khura River is much smaller, around 190  $\text{km}^2$  including tributaries. The annual precipitation around the Khura River (measured in 1997–2002 at Ranong city, nearby the watershed) ranged 3,800–5,300  $\text{mm year}^{-1}$ , which is approximately twice of that in the Trang River watershed (1,600–3,400  $\text{mm year}^{-1}$ , measured at Nakhon Si Thammarat near the upper reach and Trang city along

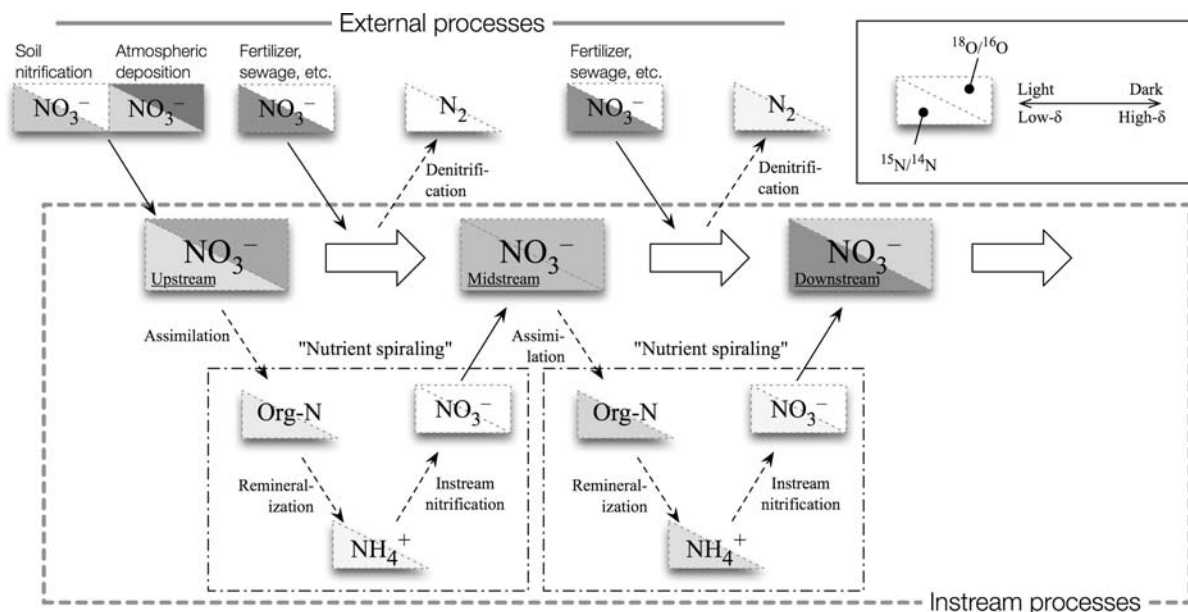
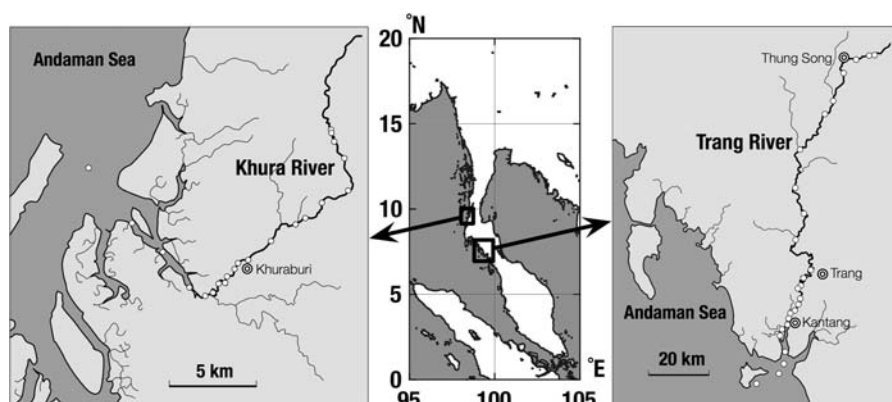


**Fig. 1** A model case of longitudinal changes in the  $\delta^{15}\text{N}$  and the  $\delta^{18}\text{O}$  of stream-water  $\text{NO}_3^-$ . Stream-water  $\text{NO}_3^-$  is a mixture of  $\text{NO}_3^-$  from different sources including atmospheric deposition, anthropogenic N loading (fertilizer, sewage, etc.), and instream nitrification. Remineralization of organic N and nitrification fractionate against  $^{15}\text{N}$  to generate  $\text{NO}_3^-$  with low  $\delta^{15}\text{N}$ , while instream denitrification and assimilative reduction also cause an elevation of  $\delta^{15}\text{N}$  of stream-water  $\text{NO}_3^-$  by their respective isotope fractionation effects. On the other hand, both the instream nitrification and the external anthropogenic

sources supply relatively  $^{18}\text{O}$ -depleted  $\text{NO}_3^-$  to the stream water, while the denitrification and the assimilation result in an elevation in the  $\delta^{18}\text{O}$  of  $\text{NO}_3^-$  left in the stream water. Atmospherically deposited  $\text{NO}_3^-$  that has typically high  $\delta^{18}\text{O}$  may affect  $\delta^{18}\text{O}$  of upstream  $\text{NO}_3^-$ . Dashed lines with arrows indicate reactions accompanied with isotope fractionation. See Discussion for details and reference materials for typical  $\delta^{15}\text{N}$  and  $\delta^{18}\text{O}$  values for each source and the magnitudes of fractionation with the reactions

**Fig. 2** Study sites, the Khura River (left) and the Trang River (right). Open circles indicate the location of sampling points. Major towns along the rivers are indicated by double circles



the lower reach in 1997–2002; GAME-T2 Data Center; [hydro.iis.u-tokyo.ac.jp/GAME-T/GAIN-T/](http://hydro.iis.u-tokyo.ac.jp/GAME-T/GAIN-T/)). Thus, the freshwater discharge through the Khura River to the sea should be several times smaller than the discharge at the gauging station of the Trang River.

## Experimental

Surface river water at the upper 11 and 12 stations of the Khura and Trang Rivers, respectively, was sampled using a bucket from bridges or by walking

into the stream, serially from upstream downwards. River water sampling at the downstream stations was conducted similarly 2 or 3 days later using a boat. Each sampling point was located using the Global Positioning System. Water temperature, pH, dissolved oxygen ( $O_2$ ) concentration, conductivity and turbidity were recorded by a portable water quality probe (WQC-22A, TOA) directly dipped in the stream. Water samples for dissolved nutrients and chloride (30 ml polypropylene (PP) bottle),  $\delta^{15}N$  and  $\delta^{18}O$  of  $NO_3^-$  (another 30 ml PP bottle), DIC concentration (20 ml screw-capped glass vial) and  $\delta^{13}C_{DIC}$  (30 ml glass vial with a butyl-rubber septum) were immediately filtered through syringe filters (ADVANTEC, cellulose-acetate membrane, 0.8  $\mu m$  pore size). Sample bottles for DIC and  $\delta^{13}C_{DIC}$  were capped without air bubbles inside. Water samples for chlorophyll *a* and particulate matter were stored temporarily in 2-L PP bottles. All the samples were transported to the laboratory on ice for further processing. Conductivity and pH of the water remaining in the bucket after subsampling were measured again and compared with the values obtained by inserting the sensor directly to the river. The two values did not differ significantly.

In the laboratory, the water samples in the 30 ml PP bottles were frozen in a freezer ( $-20^\circ C$ ) immediately. The samples for DIC and  $\delta^{13}C_{DIC}$  were amended with saturated  $HgCl_2$  solution to a final concentration of 0.01% (w/v), sealed again without air bubbles inside, and stored at room temperature. From the 2-L PP bottles, 100 ml was filtered through precombusted ( $450^\circ C$ , 3 h) glassfiber filters (Whatman GF/F, 25 mm diameter), and the filters were soaked separately in *N,N*-dimethylformamide (DMF, 6 ml) in PP tubes and stored in the dark at  $-20^\circ C$  for later analysis of chlorophyll *a*. Another 200–1,500 ml water samples were filtered through precombusted glassfiber filters (Whatman GF/F, 47 mm), and the filters were wrapped individually with aluminum foils and stored at  $-20^\circ C$  until later analysis of particulate organic carbon (POC), particulate nitrogen (PN) and their stable isotopic compositions.

Dissolved inorganic nitrogen (DIN:  $NH_4^+$ ,  $NO_2^-$  and  $NO_3^-$ ) was determined by an autoanalyzer (BLAN + LUEBBE, AACS-III). Chloride was measured for the same samples as nutrients using a

salinometer (SAT-2A, TOA) and crosschecked with the salinity data obtained by the in situ conductivity measurements.

The  $\delta^{15}N$  and  $\delta^{18}O$  of  $NO_3^-$  were determined by the denitrifier method (Sigman et al. 2001; Casciotti et al. 2002) using an isotope-ratio-monitoring mass spectrometer (IRMS) combined with purge-and-trap and prefocusing apparatus (ThermoFisher, Gas-Bench/PreCon/Delta plus XP). This analysis was executed only for the samples containing  $>1.0 \mu mol NO_3^- L^{-1}$ . The measurements were calibrated against three different reference material with distinct isotope compositions (Böhlke et al. 2003). When the  $NO_2^-/(NO_2^- + NO_3^-)$  ratio of the samples exceeded 0.05,  $NO_2^-$  was removed by reaction with ascorbic acid prior to the incubation (Granger et al. 2006).

DIC was measured by a TOC analyzer (Shimadzu, TOC-5000A).  $\delta^{13}C_{DIC}$  was determined by the head-space-equilibration method using a gas chromatograph-IRMS system (ThermoFisher, GC-6890/Combustion III/DELTA plus XP; Miyajima et al. 1995).  $pCO_2$  in estuarine waters was estimated by equilibrium calculations as follows. Dissolved  $CO_2$  concentration ( $CO_2(aq)^*$ ) was estimated from the concentration of DIC and pH using the dissociation constants of dissolved carbonate system (Millero et al. 2006) that depend on the water temperature and the salinity. Then,  $pCO_2$  was calculated by dividing  $CO_2(aq)^*$  by the solubility coefficient of gaseous  $CO_2$  (Weiss 1974) that also depends on the water temperature and the salinity.

Chlorophyll *a* concentration in DMF in which the filter samples were soaked was measured fluorometrically (Turner Designs, 10AU). POC, PN and their isotopic compositions were determined using an IRMS combined with an elemental analyzer (ThermoFisher, FLASH EA/ConFlo III/DELTA plus XP) for the 47 mm filter samples after the HCl-fuming pretreatment (Sato et al. 2006).

The carbon, nitrogen and oxygen isotopic compositions are expressed by the usual delta-notation for permil deviation from the international reference materials (i.e.  $\delta^{13}C$  vs. V-PDB,  $\delta^{15}N$  vs. atmospheric  $N_2$ , and  $\delta^{18}O$  vs. V-SMOW) throughout this paper.

Data analysis and curve fitting were executed with the aid of a software package pro Fit ver. 6.1 (QuantumSoft).



## Results

The riverbed profile of the upper reach of the Khura River (>20 km from the river-mouth station, Fig. 3a) is characterized by relatively steep longitudinal slopes. The riverbed was dominated by gravels and coarse sand, and the river water was mostly clear. The water temporarily became turbid seemingly due to the erosion of riparian fine silt between 15.7 and 10.5 km points, and also was apparently affected by effluent waters from fringing mangroves between 11.5 and 6.5 km points. These influences are reflected in the longitudinal profile of POC (Fig. 3c). The water temperature was 23.4°C at the most upstream sampling point, gradually increased to 28.0°C at the freshwater/brackish (F/B) boundary (12.8 km) and remained constant at  $29.2 \pm 0.8^\circ\text{C}$  in the saline-water section (salinity > 5; 0–10.9 km).

The Trang River has a much longer reach than the Khura River, and the riverbed slope is generally small except in the most upstream section (Fig. 3b). There is a waterfall near the riverhead, and our most upstream sampling point was located at the waterfall basin. The water temperature was 23.6°C at this point, gradually increased to 28.0°C at the F/B boundary (33 km from the river-mouth point), and

remained  $28.1 \pm 0.5^\circ\text{C}$  in the saline-water section. Although the river water was clear at a few headwater sampling points, it became somewhat turbid from 189 km down to 55 km sampling point (Fig. 3d for POC). This turbid water was presumably caused by the surface runoff from the fluvial floodplain that extended over the middle- to lower-reach watershed of the Trang River. The brackish section of the Trang River was also affected by effluents from riverside mangroves.

The dissolved oxygen ( $\text{O}_2$ ) concentration was relatively constant around 200  $\mu\text{M}$  in the upper to middle reach of both the Khura and Trang Rivers (Fig. 3a, b). It was always below saturation with respect to the atmospheric oxygen.  $\text{O}_2$  exhibited minima typically near the F/B boundary (14.5 km in the Khura River, 37 km in the Trang River) and at the center of the mangrove-affected brackish zone (9.2 km in the Khura River, 23 km in the Trang River). The DIC concentration ( $\approx 200 \mu\text{M}$ ) and the  $\delta^{13}\text{C}$  of DIC ( $\delta^{13}\text{C}_{\text{DIC}}$ ,  $\approx -15\text{‰}$ ) were stable in the upper to middle reach of the Khura River (Fig. 3e). However, DIC increased and  $\delta^{13}\text{C}_{\text{DIC}}$  dropped around the F/B boundary. In the Trang River, DIC in the most upstream section (204–189 km) was low (Fig. 3f) and  $\delta^{13}\text{C}_{\text{DIC}}$  at 204 km point was quite high ( $-7.7\text{‰}$ ).

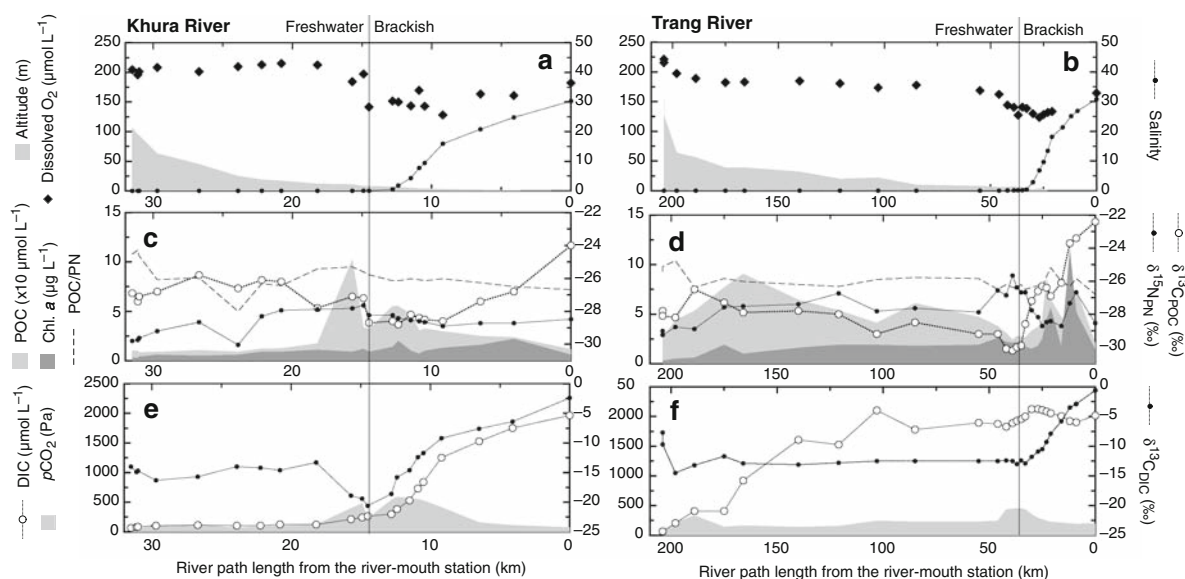


**Fig. 3** Longitudinal distribution of chemical variables along the Khura (left) and the Trang (right) Rivers. Note that the scale of x-axis is different between two rivers. Symbols: **a, b** salinity—solid circle, dissolved  $\text{O}_2$ —solid diamond, river-bed profile—shaded area; **c, d**  $\delta^{13}\text{C}_{\text{POC}}$ —open circle,  $\delta^{15}\text{N}_{\text{PN}}$ —

solid circle, POC concentration—light shaded area, chlorophyll *a* concentration—dark shaded area, POC/PN ratio—dashed line; **e, f** DIC concentration—open circle,  $\delta^{13}\text{C}_{\text{DIC}}$ —solid circle,  $\text{pCO}_2$ —shaded area. The freshwater/brackish water boundary is also indicated by vertical broken lines

However, DIC increased to  $\approx 2,000 \mu\text{mol L}^{-1}$  and  $\delta^{13}\text{C}_{\text{DIC}}$  decreased to around  $-12.5\text{‰}$  in the middle to lower reach of the Trang River. pH was relatively high in this section (7.6–7.9) compared to the upstream section of the Trang River (6.7–7.3) and the whole freshwater reach of the Khura River (6.2–7.0).  $p\text{CO}_2$  estimated by the equilibrium calculation was almost always  $>50$  Pa, well exceeding the atmospheric  $p\text{CO}_2$  (37 Pa), with only an exception at the waterfall-basin point of the Trang River ( $\approx 30$  Pa).  $p\text{CO}_2$  showed a maximum around the F/B boundary (Fig. 3e, f).

The concentration of  $\text{NO}_3^-$  was almost constant ( $\approx 5 \mu\text{M}$ ) in the upper to middle reach (31.5–18.2 km) of the Khura River (Fig. 4a). Temporary accumulation of nitrite ( $\text{NO}_2^-$ , 2.7–6.6  $\mu\text{M}$ ) was observed at 31.5, 31.0, 26.7 and 20.8 km points, while the concentration of ammonium ( $\text{NH}_4^+$ ) remained low ( $\leq 0.3 \mu\text{M}$ ). There is a small town of Khuraburi (population, ca. 11,000) at 14–15 km upstream from the river-mouth station (Fig. 2), and  $\text{NO}_3^-$  increased slightly around this town (up to 8.8  $\mu\text{M}$ ).  $\text{NH}_4^+$  increased in the oligo- and mesohaline sections of the brackish zone (12.4–10.5 km, up to 2.1  $\mu\text{M}$ ). The  $\delta^{15}\text{N}$  and  $\delta^{18}\text{O}$  of  $\text{NO}_3^-$  ( $\delta^{15}\text{N}_{\text{NO}_3}$  and  $\delta^{18}\text{O}_{\text{NO}_3}$ , Fig. 4c) as well as the  $\delta^{15}\text{N}$  of PN ( $\delta^{15}\text{N}_{\text{PN}}$ , Fig. 3c) increased throughout the freshwater reach of the Khura River. After the river water passed the F/B boundary, the  $\delta^{15}\text{N}_{\text{NO}_3}$  decreased slightly.

In the freshwater reach of the Trang River (204–55 km), the concentration of  $\text{NO}_3^-$  was relatively

constant ( $\approx 20 \mu\text{M}$ ) except at a few upstream stations (Fig. 4b). There is a large town of Trang (population, ca. 60,000) between 55 and 46 km points, and two smaller towns Thung Song (190 km, ca. 27,000) and Kantang (30 km, ca. 13,000; Fig. 2).  $\text{NO}_3^-$  increased gradually between Trang and Kantang. In the Trang River, the concentration of  $\text{NO}_2^-$  was always low ( $\leq 1 \mu\text{M}$ ), and thus the difference between DIN and  $\text{NO}_3^-$  could be ascribed largely to  $\text{NH}_4^+$ . The concentration of  $\text{NH}_4^+$  increased temporarily around Thung Song ( $\approx 12 \mu\text{M}$ ) and between Trang and Kantang (5–14  $\mu\text{M}$ ). Domestic waste water from the towns and effluent from fishworks factories of Kantang along the Trang River may have influenced DIN concentrations (Fig. 4b). The  $\delta^{15}\text{N}_{\text{NO}_3}$  (Fig. 4d) as well as the  $\delta^{15}\text{N}_{\text{PN}}$  (Fig. 3d) increased throughout the freshwater reach of the Trang River, while the  $\delta^{18}\text{O}_{\text{NO}_3}$  decreased slightly (Fig. 4d). In contrast, the  $\delta^{15}\text{N}_{\text{NO}_3}$  and the  $\delta^{15}\text{N}_{\text{PN}}$  decreased and the  $\delta^{18}\text{O}_{\text{NO}_3}$  increased across the salinity gradient of the brackish zone of the Trang River.

## Discussion

Instream metabolic activities inferred from the dynamics of DIC and  $\text{O}_2$

The watershed geology and hydrology are reflected in the profiles of DIC concentration and  $\delta^{13}\text{C}_{\text{DIC}}$

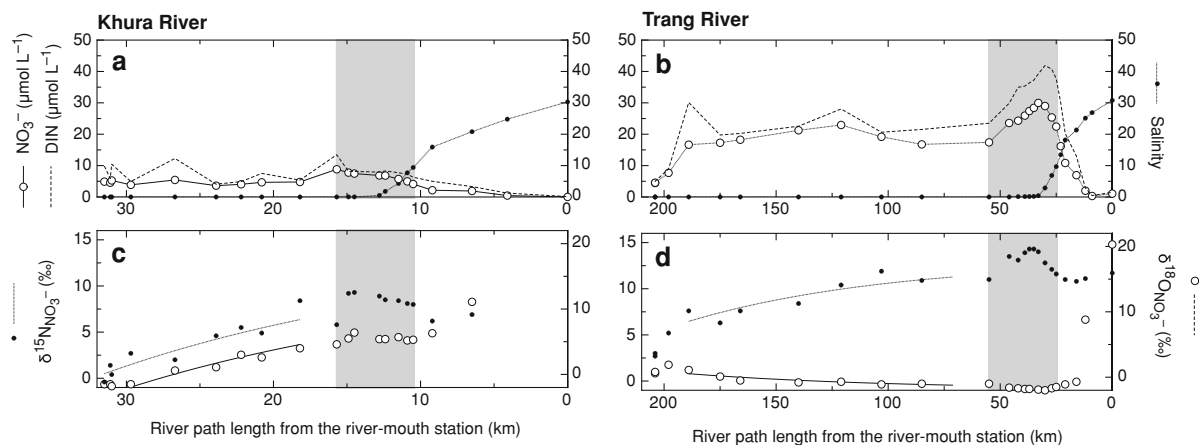


**Fig. 4** Longitudinal distribution of the concentration and the isotope composition of  $\text{NO}_3^-$  along the Khura (left) and the Trang (right) Rivers. Note that the scale of abscissa is different between two rivers. Symbols: **a, b** salinity—solid circle,  $\text{NO}_3^-$  concentration—open circle, DIN concentration—dashed line

without symbol; **c, d**  $\delta^{15}\text{N}_{\text{NO}_3}$ —solid circle,  $\delta^{18}\text{O}_{\text{NO}_3}$ —open circle. Results of the simultaneous fitting of Eq. 1 (thin solid line) and Eq. 2 (broken line) to the real data of the  $\delta^{15}\text{N}_{\text{NO}_3}$  and the  $\delta^{18}\text{O}_{\text{NO}_3}$  in the freshwater reach are also shown in **c** and **d** (see text)

(Pawellek and Veizer 1994; Kendall et al. 1995; Das et al. 2005). The watershed of the Khura River was dominated by granitic bedrocks, which is the reason for the constantly low DIC concentration in the upper to middle reach (Fig. 3e).  $\delta^{13}\text{C}_{\text{DIC}}$  around  $-15\text{‰}$  suggests that atmospheric  $\text{CO}_2$  and respiratory  $\text{CO}_2$  contributed roughly equally to the buildup of DIC (i.e. chemical weathering) in this section of the Khura River. Granitic bedrocks are also dominant in the headwater region of the Trang River, and consequently DIC in the most upstream section (204–189 km) was low (Fig. 3f). The high  $\delta^{13}\text{C}_{\text{DIC}}$  at 204 km point presumably reflected the mixing and equilibration with atmospheric  $\text{CO}_2$  due to the waterfall effect. However, DIC increased up to  $\approx 2,000 \mu\text{mol L}^{-1}$  and the  $\delta^{13}\text{C}_{\text{DIC}}$  became stable around  $-12.5\text{‰}$  in the middle to lower reach (Fig. 3f), which is ascribed to the chemical weathering of limestone that was abundant in the watershed of this section. The relatively high pH in this region is consistent with the high buffering capacity of DIC.

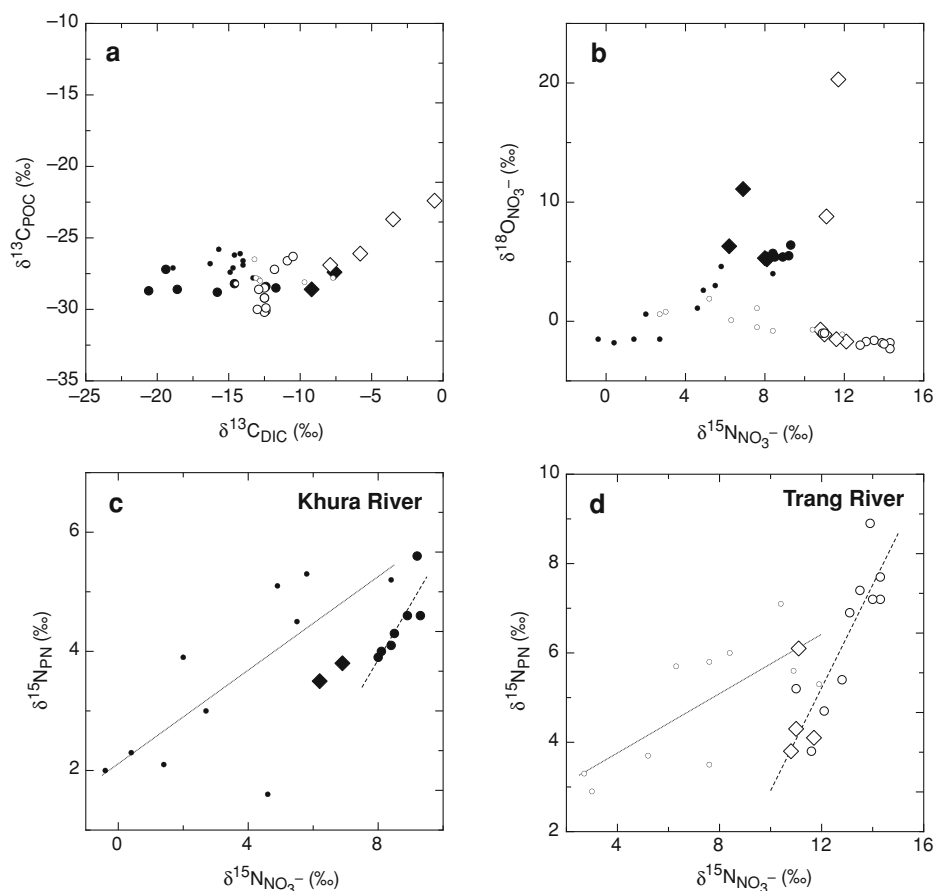
Around the freshwater/brackish (F/B) boundary (14.5 km in the Khura River, 37 km in the Trang River), the concentration of  $\text{O}_2$  and the  $\delta^{13}\text{C}$  of DIC exhibited minimal values and  $p\text{CO}_2$  had a maximum (Fig. 3a, b, e, f). The decrease of  $\delta^{13}\text{C}_{\text{DIC}}$  is indicative of elevated input of isotopically-light respiratory  $\text{CO}_2$  into river water. Such longitudinal trends of  $\text{O}_2$ ,  $p\text{CO}_2$  and  $\delta^{13}\text{C}_{\text{DIC}}$  all indicate that heterotrophic activities such as  $\text{O}_2$  consumption and  $\text{CO}_2$  production were stimulated particularly around the F/B boundary. On the other hand, the  $\delta^{13}\text{C}$  of particulate organic carbon ( $\delta^{13}\text{C}_{\text{POC}}$ ) was also conspicuously low in this zone (Fig. 3c, d). However, the absence of correlation between the  $\delta^{13}\text{C}_{\text{POC}}$  and the  $\delta^{13}\text{C}_{\text{DIC}}$  in this zone (Fig. 5a) suggests that this POC was not produced by indigenous aquatic plants within the river water but predominantly of terrestrial plant origin. It is often reported that the  $\delta^{13}\text{C}$  of natural organic matter decreases with the progress of decomposition in aquatic environments (Fenton and Ritz 1988; Lehmann et al. 2002), supposedly due to the selective remineralization of relatively  $^{13}\text{C}$ -enriched fractions such as carbohydrates and proteins leaving behind insoluble,  $^{13}\text{C}$ -depleted fractions such as lignin and lipids. Therefore, the low  $\delta^{13}\text{C}_{\text{POC}}$  around the F/B boundary may be indicative of accumulation of aged detrital organic matter. The enhanced heterotrophic activity around the F/B boundary has

been reported for major temperate rivers and ascribed to the accumulation and the active decomposition of river-borne labile POC in this zone (Frankignoulle et al. 1998). The above findings suggest that the function of the F/B boundary in the carbon cycle is similar between temperate and tropical rivers.

In contrast to the F/B boundary where the detrital organic matter transported by river water contributes predominantly to the instream metabolic activities, the brackish zone often receives an enormous input of both organic and inorganic carbon from tidal wetlands such as salt marsh and mangrove (Cai et al. 2003; Neubauer and Anderson 2003; Bouillon et al. 2008). This allochthonous carbon input can strongly affect the water chemistry and the instream metabolic processes in this zone. The second minimum in the longitudinal  $\text{O}_2$  profile that was evident at around 9.2 km point of the Khura River (salinity 15.9; Fig. 3a) and 23 km point of the Trang River (salinity 13.5; Fig. 3b) is an indication of this effect. It can be recognized also in the profile of  $\delta^{13}\text{C}_{\text{DIC}}$ . Although the  $\delta^{13}\text{C}_{\text{DIC}}$  in the saline-water section rapidly increased due to the mixing with isotopically heavier marine DIC (Fig. 3e, f), mass-balance calculations have demonstrated that the measured  $\delta^{13}\text{C}$  in this zone was significantly deviated negatively by up to 5.7 and 2.4‰ in the Khura and Trang Rivers, respectively, from the values that were expected by the conservative mixing of river and marine DIC (Miyajima et al. 2009). These characteristic profiles apparently reflect the influence of the mangroves that were abundant in the intertidal area along the estuary of the Khura and Trang Rivers.

In view of the above findings, we discuss the biogeochemical nitrogen cycling separately in the following sections: (1) the freshwater reach, (2) the freshwater/brackish (F/B) transition zone and (3) the saline-water section of the Khura and Trang Rivers. In the freshwater reach, the concentrations of  $\text{O}_2$ , DIC, and  $\text{NO}_3^-$  were relatively constant except for a few upstream sampling points in the Trang River, indicating quasi-steady-state turnover of these constituents. In the F/B transition zone and the saline-water section, instream heterotrophic activities were enhanced by accumulation of terrestrial and mangrove-derived labile POC, respectively, and consequently turnover of  $\text{NO}_3^-$  was highly dynamic. The influence of domestic wastewater inputs could also be significant in the F/B transition zone, where the watershed was densely populated.





Khura	Trang		Khura River	Trang River
•	○	Freshwater reach		
●	○	F/B boundary zone	Freshwater reach: $\delta^{15}\text{N}_{\text{PN}} = 0.39 \cdot \delta^{15}\text{N}_{\text{NO}_3^-} + 2.11$	$\delta^{15}\text{N}_{\text{PN}} = 0.33 \cdot \delta^{15}\text{N}_{\text{NO}_3^-} + 2.43$
◆	◇	Saline-water section	F/B boundary zone: $\delta^{15}\text{N}_{\text{PN}} = 0.92 \cdot \delta^{15}\text{N}_{\text{NO}_3^-} - 3.57$	$\delta^{15}\text{N}_{\text{PN}} = 1.15 \cdot \delta^{15}\text{N}_{\text{NO}_3^-} - 8.60$

**Fig. 5** Relationships between  $\delta^{13}\text{C}_{\text{DIC}}$  and  $\delta^{13}\text{C}_{\text{POC}}$  (a),  $\delta^{15}\text{N}_{\text{NO}_3^-}$  and  $\delta^{18}\text{O}_{\text{NO}_3^-}$  (b), and between  $\delta^{15}\text{N}_{\text{NO}_3^-}$  and  $\delta^{15}\text{N}_{\text{PN}}$  (c, d). Linear regression lines of  $\delta^{15}\text{N}_{\text{PN}}$  to  $\delta^{15}\text{N}_{\text{NO}_3^-}$  for the

freshwater reach (solid line) and the freshwater/brackish boundary zone (dashed line) are shown with formulae in the box below the plots

#### Turnover of $\text{NO}_3^-$ in the freshwater reach

The upper to middle reach of the Khura River and the middle to lower reach of the Trang Rivers are net heterotrophic systems as indicated by slightly undersaturated  $\text{O}_2$  concentrations, supersaturated  $p\text{CO}_2$ , and the  $\delta^{13}\text{C}$  of DIC that was kept constantly lower than the atmospheric equilibrium value (−4 to +1‰ depending on pH). Remarkably constant longitudinal distributions of  $\text{O}_2$ ,  $p\text{CO}_2$ ,  $\delta^{13}\text{C}_{\text{DIC}}$  as well as the concentration of  $\text{NO}_3^-$  suggest that instream metabolic activities involved in C and N turnover were nearly in steady state in this section. The roughly

constant distribution of  $\text{NO}_3^-$  (Fig. 4a, b) may be a result of either (1) conservative transport of  $\text{NO}_3^-$  by rivers with little influences of instream metabolic activities, or (2) dynamic balance between the inputs (instream nitrification and external loading) and the outputs (denitrification and assimilation) of  $\text{NO}_3^-$  within the river channel. If the conservative transport had been the dominant process compared to the instream turnover of  $\text{NO}_3^-$ , then the stable isotope composition of  $\text{NO}_3^-$  should have barely changed throughout the reaches. In fact, the  $\delta^{15}\text{N}_{\text{NO}_3^-}$  consistently increased across the freshwater reach of both the Khura River (from −0.4 to +9.3‰; Fig. 4c) and

the Trang River (from +2.7 to +13.5‰; Fig. 4d). The  $\delta^{18}\text{O}_{\text{NO}_3}$  also changed longitudinally: an increasing trend similar to the  $\delta^{15}\text{N}_{\text{NO}_3}$  was found in the Khura River (from -1.8 to +6.4‰; Fig. 4c), whereas the  $\delta^{18}\text{O}_{\text{NO}_3}$  was slightly decreased in the Trang River (from +1.9‰ to -1.8‰; Fig. 4d). These observations indicate that  $\text{NO}_3^-$  in these river waters was gradually replaced by isotopically different  $\text{NO}_3^-$ , and that the apparently constant  $\text{NO}_3^-$  concentrations were kept by the dynamic balance between the inputs and the outputs of  $\text{NO}_3^-$ .

The longitudinal changes in  $\delta^{15}\text{N}_{\text{NO}_3}$  and  $\delta^{18}\text{O}_{\text{NO}_3}$  may be caused by several mechanisms, including (1) internal removal processes of  $\text{NO}_3^-$ , such as denitrification and assimilation, associated with isotope fractionation, (2) internal production by nitrification of  $\text{NO}_3^-$  isotopically different from the preexisting  $\text{NO}_3^-$ , and (3) external loading of isotopically-different  $\text{NO}_3^-$  from the watershed. The fact that  $\text{NO}_3^-$  concentration in the freshwater reach of the Khura and Trang Rivers was largely constant implies that  $\text{NO}_3^-$  was removed and simultaneously compensated by the instream nitrification and/or the external loading. In the following, we briefly review the patterns of  $\delta^{15}\text{N}_{\text{NO}_3}$  and  $\delta^{18}\text{O}_{\text{NO}_3}$  potentially created by these processes (Fig. 1).

The reductive removal of  $\text{NO}_3^-$  due to denitrification and assimilation is accompanied with N and O isotope fractionations. The magnitude of isotope fractionation ( $^{15}\epsilon$  or  $^{18}\epsilon$ , defined here as the average  $\delta^{15}\text{N}$  or  $\delta^{18}\text{O}$  of existing  $\text{NO}_3^-$  pool minus the  $\delta^{15}\text{N}$  or  $\delta^{18}\text{O}$  of  $\text{NO}_3^-$  just being removed by reduction, respectively) depends on specific processes. In the case of the assimilatory  $\text{NO}_3^-$  reduction by microalgae,  $^{15}\epsilon$  is generally small ranging 0–10‰ (usually <5‰; Montoya and McCarthy 1995; Needoba et al. 2003). In contrast, the dissimilatory  $\text{NO}_3^-$  reduction by denitrifiers potentially causes a large fractionation ( $^{15}\epsilon$  up to 40‰, but often around 25‰; Mariotti et al. 1981; Kendall et al. 2007). Although the estimation of  $^{18}\epsilon$  has been relatively scarce compared to  $^{15}\epsilon$ , existing reports generally indicate that  $^{18}\epsilon$  for  $\text{NO}_3^-$  reduction processes is not largely different from  $^{15}\epsilon$ , with the  $^{15}\epsilon/^{18}\epsilon$  ratio mostly falling between 0.8 and 2.0 (Lehmann et al. 2003; Granger et al. 2004; Sigman et al. 2005). The magnitude of the apparent isotope fractionation also depends on physical environments. The apparent  $^{15}\epsilon$  associated with the DIN assimilation decreases when the stream water

velocity is so low that the thick boundary layer created around the periphyton strongly restricts the diffusion of DIN (Trudeau and Rasmussen 2003). The apparent  $^{15}\epsilon$  of denitrification diminishes similarly when the denitrification in the river beds proceeded under diffusion-limited conditions and the intrinsic isotope effect of denitrification was not be fully realized in the  $\delta^{15}\text{N}$  values of  $\text{NO}_3^-$  left behind in river water (Sigman et al. 2003; Ruehl et al. 2007).

The  $\delta^{15}\text{N}$  of  $\text{NO}_3^-$  produced by instream nitrification is principally constrained by the  $\delta^{15}\text{N}$  of organic matter subject to remineralization. The aerobic remineralization of organic matter is usually accompanied with a small isotope fractionation, and results in  $\text{NH}_4^+$  with 0–4‰ lower  $\delta^{15}\text{N}$  than the bulk original organic matter (Lehmann et al. 2002; Dijkstra et al. 2008; C. Yoshimizu, unpublished data). Nitrification of  $\text{NH}_4^+$  to  $\text{NO}_3^-$  is associated intrinsically with a large isotope discrimination (14–38‰; Casciotti et al. 2003), although it may not be evident in  $\delta^{15}\text{N}_{\text{NO}_3}$  in river water when the remineralization and the nitrification proceed nearly in the steady state. Specifically in the case of the Khura and Trang Rivers, the  $\delta^{15}\text{N}$  of particulate nitrogen ( $\delta^{15}\text{N}_{\text{PN}}$ ) was  $+3.3 \pm 1.4$  and  $+5.5 \pm 1.0$ ‰ (average  $\pm$  SD) in the freshwater reach of the Khura and Trang Rivers, respectively (Fig. 3c, d). Given that  $\delta^{15}\text{N}_{\text{PN}}$  represents the  $\delta^{15}\text{N}$  of decomposing organic matter in rivers and that the combined isotope effect of remineralization and nitrification can be scaled to be 3‰ or greater,  $\delta^{15}\text{N}_{\text{NO}_3}$  due to instream nitrification in the Khura and Trang Rivers may be expected to be lower than +0.3 and +2.5‰, respectively.

On the other hand, it is empirically recognized that  $\text{NO}_3^-$  produced by nitrification in aquatic environments usually takes similar  $\delta^{18}\text{O}$  values to the ambient water (Casciotti et al. 2002; Sigman et al. 2005; our unpublished data in a freshwater lake). This has been ascribed principally to the rapid exchange of O atoms between nitrification intermediates (e.g.  $\text{NO}_2^-$ ) and ambient water molecules catalyzed by the nitrification-related enzymes (Kool et al. 2007), although the exact mechanisms responsible for the lack of fractionation remain to be demonstrated.

There are various external sources of  $\text{NO}_3^-$  to river waters, including  $\text{NO}_3^-$  derived from natural  $\text{N}_2$  fixation followed by remineralization and nitrification in the watershed soils, that derived from atmospheric

deposition of nitrogen oxides in the watershed, and anthropogenic  $\text{NO}_3^-$  derived from manures, fertilizers, septic and animal waste, and domestic and industrial wastewaters, which have diverse  $\delta^{15}\text{N}$  and  $\delta^{18}\text{O}$  values depending on sources (Kendall et al. 2007). However,  $\text{NO}_3^-$  derived from manure and septic and animal waste has typically high  $\delta^{15}\text{N}$  ( $\approx +10\text{‰}$  or higher; Bedard-Haughn et al. 2003). Domestic waste water input also generally increases  $\delta^{15}\text{N}_{\text{NO}_3}$  in river water (McClelland and Valiela 1998). As  $\text{NO}_3^-$  from these origins is produced via nitrification, its  $\delta^{18}\text{O}$  would not be very different from ambient water. Denitrification in soils and aquifers may increase  $\delta^{15}\text{N}_{\text{NO}_3}$  and  $\delta^{18}\text{O}_{\text{NO}_3}$  during transportation, typically with a ratio of 2:1 (Kendall et al. 2007). In contrast,  $\text{NO}_3^-$  from atmospheric deposition shows very high  $\delta^{18}\text{O}$  ( $>+60\text{‰}$ ).

Thus, the instream processes and the external sources that are responsible for the turnover of  $\text{NO}_3^-$  in a given river may be discerned if the magnitude of the isotope fractionation due to the removal process and the  $\delta^{15}\text{N}$  of  $\text{NO}_3^-$  newly added to the river water could be determined, respectively. Specifically, an estimated  $^{15}\epsilon$  much larger than  $10\text{‰}$  would indicate denitrification as the dominant removal process of  $\text{NO}_3^-$ , while smaller  $^{15}\epsilon$  values suggest that the river-water  $\text{NO}_3^-$  is removed mainly by assimilation or otherwise by denitrification under diffusion-limited conditions. On the other hand, the  $\delta^{15}\text{N}$  of newly-added  $\text{NO}_3^-$  similar to or lower than the  $\delta^{15}\text{N}$  of PN suggests that instream nitrification is a candidate for the dominant source of  $\text{NO}_3^-$ . If the  $\delta^{15}\text{N}$  of newly-added  $\text{NO}_3^-$  is estimated to be much higher, the external loading of the wastewater  $\text{NO}_3^-$  would be a feasible source. In the following, we introduce a simple procedure to estimate these values using the longitudinal distributions of the  $\delta^{15}\text{N}$  and  $\delta^{18}\text{O}$  of  $\text{NO}_3^-$  in river channels in which the quasi-steady-state turnover of  $\text{NO}_3^-$  can be assumed.

#### A steady-state turnover model of river-water $\text{NO}_3^-$

When  $\text{NO}_3^-$  in the river water is constantly removed by reduction and compensated by internal nitrification and/or external loading at a fixed rate of, say,  $r \mu\text{mol L}^{-1} \text{ km}^{-1}$  keeping the  $\text{NO}_3^-$  concentration at  $C \mu\text{mol L}^{-1}$ , the spiraling length of  $\text{NO}_3^-$  is evaluated by the ratio  $C/r$ . The concept of spiraling length

has long been used to evaluate instream biogeochemical activities for important nutrient elements and compare them between rivers and between different nutrients (Fisher et al. 2004). If the isotope fractionation associated with the removal process ( $^{15}\epsilon$ ,  $^{18}\epsilon$ ) and the average nitrogen and oxygen isotope compositions of  $\text{NO}_3^-$  being added ( $^{15}\delta_0$  and  $^{18}\delta_0$ , respectively) can be assumed to be constant within a given section of a river, the longitudinal distribution of  $\delta^{15}\text{N}_{\text{NO}_3}$  and  $\delta^{18}\text{O}_{\text{NO}_3}$  in the section can be expressed by the following functions:

$$\delta^{15}\text{N}_{\text{NO}_3}(x) = -\left(^{15}\epsilon + ^{15}\delta_0 - \delta^{15}\text{N}_{\text{NO}_3}(0)\right) \times \exp(-x/L) + ^{15}\epsilon + ^{15}\delta_0 \quad (1)$$

$$\delta^{18}\text{O}_{\text{NO}_3}(x) = -\left(^{18}\epsilon/k + ^{18}\delta_0 - \delta^{18}\text{O}_{\text{NO}_3}(0)\right) \times \exp(-x/L) + (^{15}\epsilon/k) + ^{18}\delta_0 \quad (2)$$

where  $x$  is the river-path length measured from the upstream end of the stream section,  $k$  represents the ratio  $^{15}\epsilon/^{18}\epsilon$ , and  $L$  is the spiraling length (km).

This model is tentatively applied to explain the longitudinal changes in  $\delta^{15}\text{N}_{\text{NO}_3}$  and  $\delta^{18}\text{O}_{\text{NO}_3}$  along the freshwater section of the Khura and Trang Rivers. Specifically, we assumed  $k$  to be 1. The value of  $^{18}\delta_0$  was assumed here to be constant and identical to the  $\delta^{18}\text{O}$  of the ambient water, and the latter was further assumed to be identical to that of the average meteoric water around the study site ( $-5.0\text{‰}$ ; Clark and Fritz 1997). Then, the parameters  $^{15}\epsilon$ ,  $^{15}\delta_0$  and  $L$  were adjusted so that the above two functions may simultaneously fit to the present dataset. For the Khura River, all the points in the freshwater reach (31.5–18.2 km) were used for fitting (Fig. 4c). For the Trang River, the data from between 189 and 85 km points were used (Fig. 4d).

In the case of the Khura River,  $^{15}\epsilon$  ( $=^{18}\epsilon$  in this case) was evaluated to be a relatively large value of  $16.3\text{‰}$ , reflecting conspicuous longitudinal increase of both  $\delta^{15}\text{N}_{\text{NO}_3}$  and  $\delta^{18}\text{O}_{\text{NO}_3}$  (Fig. 4c). This is much larger than  $^{15}\epsilon$  known for assimilatory  $\text{NO}_3^-$  reduction and thus indicates that denitrification would have operated as the predominant removal process in this river. The average  $\delta^{15}\text{N}$  of  $\text{NO}_3^-$  added to the river ( $^{15}\delta_0$ ) was evaluated to be  $-1.8\text{‰}$ , which is not an unrealistic value for  $\delta^{15}\text{N}_{\text{NO}_3}$  due to instream nitrification ( $\leq +0.3\text{‰}$ ). Such a low  $^{15}\delta_0$  indicates that anthropogenic  $\text{NO}_3^-$  loading to this river was

insignificant, as also expected from relatively small population in the watershed.

In the Trang River,  $^{15}\epsilon$  ( $=^{18}\epsilon$ ) was evaluated to be as small as 3.1‰, which is a result of the slightly declining longitudinal change of  $\delta^{18}\text{O}_{\text{NO}_3^-}$  (Fig. 4d). This apparently implies that the removal process of  $\text{NO}_3^-$  in this river was predominated by the assimilatory reduction by primary producers and bacteria, rather than denitrification, and this interpretation seems consistent with the fact that most of the freshwater reach of the Trang River was open to the insolation that would promote primary production within the river. However, such a small  $^{15}\epsilon$  may have also been realized if denitrification in the river beds proceeded under diffusion-limited conditions. In fact, the riverbed slope was relatively small and the riverbed was extensively covered with fine silt in the Trang River compared to the Khura River. Such conditions may have restricted hydraulic conductivity to the hyporheic layer and forced the denitrification in this layer to proceed under diffusion-limited conditions (Grimaldi and Chaplot 2000).  $^{15}\delta_0$  in the Trang River was evaluated to be +9.9‰, which is considerably higher than the range of  $\delta^{15}\text{N}$  expected for  $\text{NO}_3^-$  produced by the instream nitrification ( $\leq +2.5\text{‰}$ ).

The contrasting longitudinal trends of  $\delta^{15}\text{N}_{\text{NO}_3^-}$  and  $\delta^{18}\text{O}_{\text{NO}_3^-}$  in the Trang River (Fig. 4d) suggests that the isotope fractionation of the removal process may not be identical between N and O but much larger for N than O. Indeed, apparent  $^{15}\epsilon/^{18}\epsilon$  ratios as large as 2 have been reported especially in freshwater environments, possibly reflecting the difference in enzyme systems mediating the denitrification process (Kendall et al. 2007). Thus, we reevaluated  $^{15}\epsilon$  and  $^{15}\delta_0$  under the constraint of  $k = 2$ . However, the results were essentially same as before; that is, the reevaluated  $^{15}\epsilon$  (6.3‰) was within the range of fractionation associated with the assimilatory reduction and the diffusion-limited denitrification, and  $^{15}\delta_0$  (+6.8‰) was out of the range of  $\delta^{15}\text{N}_{\text{NO}_3^-}$  expected for instream nitrification. The high  $^{15}\delta_0$  suggests that external loading of  $^{15}\text{N}$ -enriched anthropogenic  $\text{NO}_3^-$  was primarily responsible for the replenishment of  $\text{NO}_3^-$  in the Trang River, which is again consistent with relatively eutrophic state of this river as mentioned earlier.

The spiraling length of  $\text{NO}_3^-$  in the Khura and Trang Rivers was estimated to be ca. 24 and 90 km,

respectively. These estimates are much longer than the spiraling lengths for  $\text{NO}_3^-$  ever estimated in various streams and rivers (typically  $\leq 5$  km; Ensign and Doyle 2006). The potential reactivity of the riverbed with respect to the N turnover may be represented better by the “uptake velocity” that corresponds to the concentration-normalized uptake rate of  $\text{NO}_3^-$  per unit area of the riverbed and is equal to the river discharge rate divided by the spiraling length and the channel width. Although the exact discharge rates are unknown, the previously estimated average discharge rate for the Trang River in December ( $98.6 \text{ m}^3 \text{ s}^{-1}$ ; Vörösmarty et al. 1996) and the channel width of 50 m (typical to the middle reach of the Trang River) may be tentatively applied to calculate the uptake velocity of the Trang River, which results in  $1.3 \text{ mm min}^{-1}$ . This estimate is within the interquartile range (0.5–4.3), though considerably smaller than the average (3.7), of the previous estimates of the uptake velocity compiled by Ensign and Doyle (2006). The exceptionally long spiraling lengths of  $\text{NO}_3^-$  in the Khura and Trang Rivers may be ascribed to particularly high discharge rates (and consequently high flow speeds) of these rivers in the observed periods, as well as to the large channel dimensions of these rivers compared to many of the previously investigated streams. However, the assumption used in the model (Eqs. 1, 2) might have caused an overestimation of the spiraling length (and consequently an underestimation of the uptake velocity). In this model,  $\text{NO}_3^-$  produced by nitrification within the rivers was assumed to have constant  $\delta^{15}\text{N}$  and  $\delta^{18}\text{O}$  values (i.e.  $^{15}\delta_0$  and  $^{18}\delta_0$ ) throughout the river path. In fact, the  $\delta^{15}\text{N}$  of PN was found to increase consistently along the river path of both the Khura and Trang Rivers (Fig. 3c, d; see below), which may imply that  $\text{NO}_3^-$  produced within the rivers through the remineralization of PN coupled to the nitrification should have also been gradually enriched with  $^{15}\text{N}$ . If this is the case, the model that assumes a constant  $^{15}\delta_0$  would overestimate the spiraling length. Therefore, for estimating spiraling length accurately, model should consider at least the variability of  $^{15}\delta_0$ .

Apart from the variability of the  $\delta^{15}\text{N}$  of PN, some other uncertainties may affect the model estimates. First, the assumption that the  $\delta^{18}\text{O}$  of  $\text{NO}_3^-$  produced by the nitrification is equal to the  $\delta^{18}\text{O}$  of the ambient water relies only on an empirical relationship and has

not been substantiated mechanistically. It is possible that the  $\delta^{18}\text{O}$  of the nitrification-derived  $\text{NO}_3^-$  is considerably higher than the ambient water when the exchange of oxygen atoms between nitrification intermediates and the ambient water is limited by some environmental conditions (Kool et al. 2007). Second, the  $\delta^{18}\text{O}$  of the externally loaded  $\text{NO}_3^-$ , which was assumed here to be identical to  $^{18}\delta_0$ , may be significantly higher than the  $\text{NO}_3^-$  produced by the instream nitrification, owing to the isotope fractionation associated with denitrification during transport toward the river. Third, the variability of the magnitude of the apparent isotope fractionation associated with instream nitrification affects the validity of the assumption of the constant  $^{15}\delta_0$ . In fact, the concentration of  $\text{NO}_2^-$  was elevated at several sampling points in the Khura River (31.5, 31.0, 26.7 and 20.8 km), and at these points, the  $\delta^{15}\text{N}_{\text{NO}_3}$  was somewhat lower than the best-fit curve in Fig. 4c. This may be a result of the isotope fractionation that was made apparent by the incomplete oxidation of  $\text{NO}_2^-$ , and in such cases, the  $^{15}\delta_0$  value should be considered to be lower than the other cases. Finally,  $\text{NO}_3^-$  from atmospheric deposition, which was ignored in the above model, may significantly affect the  $\delta^{15}\text{N}$  and especially the  $\delta^{18}\text{O}$  of river-water  $\text{NO}_3^-$  when the precipitation is intense. When significant influences of these factors are expected, further refinements of the model are needed to infer correctly the contributions of the major internal and external processes to the dynamics of river-water  $\text{NO}_3^-$ .

#### N turnover in the freshwater/brackish transition zone

The freshwater/brackish (F/B) transition zone is defined here as the section in which the altitude is already lower than 10 m but the salinity was still below 10. Such zones corresponded to 15.7–10.5 km section of the Khura River and 55–25 km section of the Trang River (Fig. 4). The higher concentration of  $\text{NO}_3^-$  as well as DIN in this zone than the freshwater reach (Fig. 4a, b) indicates that the internal production and/or the external loading of  $\text{NO}_3^-$  exceeded the internal removal. However,  $\text{NO}_3^-$  rapidly decreased after the river water passed the F/B boundary, which is primarily ascribed to the dilution by mixing with  $\text{NO}_3^-$ -depleted seawater. The

$\delta^{15}\text{N}_{\text{NO}_3}$  exhibited a maximal value at the F/B boundary of both the Khura River (+9.3‰ at 14.5 km; Fig. 4c) and the Trang River (+14.3‰ at 35 km; Fig. 4d).  $\delta^{18}\text{O}_{\text{NO}_3}$  also had a maximal value in the Khura River (+6.4‰) but a minimal value in the Trang River (−2.3‰) at the same points.

The increase of  $\delta^{15}\text{N}_{\text{NO}_3}$  in both rivers and  $\delta^{18}\text{O}_{\text{NO}_3}$  in the Khura River as well as the decrease in  $\delta^{18}\text{O}_{\text{NO}_3}$  in the Trang River towards the F/B boundary can be explained essentially by the same mechanism as in the freshwater reach of these rivers. In contrast, in the section downstream of the F/B boundary, the  $\delta^{15}\text{N}_{\text{NO}_3}$  slightly decreased and the  $\delta^{18}\text{O}_{\text{NO}_3}$  slightly increased, which can not be explained by the above mechanism. This trend was especially evident in the Trang River (Fig. 4d, Fig. 5b). Mixing with seawater would not explain this trend, because  $\text{NO}_3^-$  was almost depleted in seawater off the Khura as well as Trang River mouth and thus mixing with seawater would not affect  $\delta^{15}\text{N}_{\text{NO}_3}$  and  $\delta^{18}\text{O}_{\text{NO}_3}$  in brackish waters. One possible mechanism of the decrease of  $\delta^{15}\text{N}$  is production of  $^{15}\text{N}$ -depleted  $\text{NO}_3^-$  by the nitrification in estuarine waters. In the F/B transition zone,  $\text{NH}_4^+$  was accumulated up to 2.1 and 14.4  $\mu\text{mol L}^{-1}$  in the Khura and Trang River estuaries, respectively, presumably due to the active remineralization of accumulated detrital organic matter. Effluents of domestic and industrial wastewater might have also contributed to the buildup of  $\text{NH}_4^+$  especially in the Trang River. Since the nitrification in brackish waters is potentially accompanied with a large N isotope fractionation (up to 25‰; Sugimoto et al. 2008), partial oxidation of  $\text{NH}_4^+$  by the nitrification could generate highly  $^{15}\text{N}$ -depleted  $\text{NO}_3^-$ . On the other hand,  $\text{NO}_3^-$  produced by the nitrification usually has similar  $\delta^{18}\text{O}$  values to the ambient water. The  $\delta^{18}\text{O}$  of the estuarine water is expected to increase along with salinity because the  $\delta^{18}\text{O}$  of seawater ( $\approx 0\text{‰}$ ) is higher than that of river water ( $\approx -5\text{‰}$ ). Therefore, if  $\text{NO}_3^-$  preexisting in estuarine water has  $\delta^{18}\text{O}$  significantly lower than 0‰ as in the case of the Trang River,  $\delta^{18}\text{O}_{\text{NO}_3}$  should increase as original  $\text{NO}_3^-$  is gradually replaced with  $\text{NO}_3^-$  that is newly produced in situ by the nitrification. Thus, the declining  $\delta^{15}\text{N}_{\text{NO}_3}$  and increasing  $\delta^{18}\text{O}_{\text{NO}_3}$  trends seen in the oligohaline section imply that  $\text{NO}_3^-$  in this section was not simply diluted by the mixing with seawater but actively turned over by internal recycling processes.



The internal transformation of N within the river channel can occur also between DIN and PN through the assimilation/remineralization cycle. The C/N ratio of particulate organic matter (POM) suspended in river waters is usually much lower than that typical to terrestrial plant tissues as in the case of the Khura and Trang Rivers (Fig. 3c, d), which suggests that the river POM consists of a mixture of microbially reworked detrital organic matter and microbial cells produced within the river, rather than simple fragments of terrestrial plant tissues. In fact, the  $\delta^{15}\text{N}$  of PN in river water is not only constrained by the  $\delta^{15}\text{N}$  of source organic matter but gradually changes toward the  $\delta^{15}\text{N}$  of DIN in the same river water, principally due to incorporation of DIN to suspended particles by the instream primary production of microalgae as well as the secondary production of particle-attached bacteria (Finlay and Kendall 2007). Thus, the relative influence of the coupled assimilation/remineralization cycle on the turnover of PN in the river water may be evaluated by the degree of correspondence of the longitudinal  $\delta^{15}\text{N}$  between PN and DIN.

Such correlation was found even in the freshwater reach of the Khura and Trang Rivers where both the  $\delta^{15}\text{N}_{\text{NO}_3^-}$  and the  $\delta^{15}\text{N}_{\text{PN}}$  gradually increased downstream (Fig. 3c, d). However, the longitudinal increase of  $\delta^{15}\text{N}_{\text{PN}}$  was much smaller than that of  $\delta^{15}\text{N}_{\text{NO}_3^-}$ , as illustrated by the slope of regression line of  $\delta^{15}\text{N}_{\text{PN}}$  to  $\delta^{15}\text{N}_{\text{NO}_3^-}$  as low as 0.39 and 0.33 in the Khura and Trang Rivers, respectively (Fig. 5c, d). This result implies that, although the incorporation of DIN contributed significantly to the buildup of PN pool in river water, N contained in the original source organic matter was also preserved during transportation. In contrast, correlation of these two parameters was apparently much stronger and the slope of regression was close to 1 (0.92 in the Khura River and 1.15 in the Trang River) in the F/B transition zone (Fig. 5c, d). Both the values simultaneously increased at first and then simultaneously decreased as the river water passed the F/B boundary. This fact suggests that PN in the F/B transition zone was turned over through the assimilation and the regeneration of  $\text{NO}_3^-$  within a relatively short interval of river channel. Such an active turnover would be a result of both high heterotrophic activities as demonstrated earlier by the DO,  $p\text{CO}_2$  and  $\delta^{13}\text{C}_{\text{DIC}}$  trends, and the longer residence time of river water in this zone compared to the freshwater reach.

The F/B transition zone has been recognized as a hotspot in the whole-river scale in terms of the biogeochemical carbon cycle and the  $\text{CO}_2$  emission to the atmosphere (Frankignoulle et al. 1998). The present study illustrated that this view can be also applied to the nitrogen cycle, particularly internal turnover of organic and inorganic nitrogen.

#### DIN turnover in the saline-water section

As discussed earlier, the mesohaline and polyhaline sections of the brackish zone of both the Khura and Trang Rivers are characterized by conspicuous fluxes of DIC and POC from the fringing mangroves. It may be expected that the high heterotrophic activities should have coincided with active remineralization of organic nitrogen and regeneration of DIN in the estuarine water. However, no sign of DIN regeneration was observed in the longitudinal distribution of  $\text{NO}_3^-$  and  $\text{NH}_4^+$ .  $\text{NO}_3^-$  decreased almost linearly with increasing salinity (Fig. 4a, b), suggesting that  $\text{NO}_3^-$  was mostly constrained by the conservative dilution by the mixing with seawater. The  $\text{NH}_4^+$  concentration exhibited a maximum in the section of salinity 5–10, and then almost linearly decreased with salinity. In the Trang River,  $\text{NH}_4^+$  did not simply decrease by the dilution but was also apparently consumed within the polyhaline section and almost depleted at 9 km point (salinity 26.9). This consumption of  $\text{NH}_4^+$  is ascribed to the uptake by estuarine phytoplankton, as suggested by conspicuous accumulation of chlorophyll *a* at 21 and 12 km points (Fig. 3d). These results imply contrasting effects of the riverside mangroves on the C and N cycles of the estuary. The mangrove exerts a marked influence on the chemistry of carbon by exporting large amounts of organic and inorganic carbon to the estuary, but the export flux of inorganic nitrogen to estuarine waters is virtually absent. Such biogeochemical characteristics of the tidal wetlands have been reported for both salt marsh and mangrove (Cai et al. 2000; Holmer 2003) and are explained as follows. The highly C-rich nature of organic matter produced within the wetland ecosystem as well as the oligotrophic conditions that generally prevail in these areas forces the remineralization processes to proceed under N-limited conditions. Consequently, DIN is barely regenerated but even immobilized by bacterial secondary production in the course of decomposition of wetland-derived organic matter.

However, the longitudinal changes of the  $\delta^{15}\text{N}_{\text{NO}_3}$  and the  $\delta^{18}\text{O}_{\text{NO}_3}$  reveal a different aspect of the nitrogen cycle in the saline-water section. The  $\delta^{15}\text{N}_{\text{NO}_3}$  consistently decreased in the oligohaline and mesohaline sections until it reached a minimum at 9.2 km point of the Khura River (salinity 15.9) and 16 km point of the Trang River (salinity 21.3), and then was kept almost constant or slightly increased in the polyhaline section (Fig. 4c, d). This declining trend could be ascribed to nitrification in estuarine waters as discussed earlier. In contrast, the  $\delta^{18}\text{O}_{\text{NO}_3}$  increased throughout the estuary, and the rate of increase became greater especially in the polyhaline section. These facts imply that  $\text{NO}_3^-$  was not simply diluted across the salinity gradient but some chemical and/or biochemical processes influenced the behavior of  $\text{NO}_3^-$ , particularly its  $\delta^{18}\text{O}$ .

To date, the increase of the  $\delta^{18}\text{O}_{\text{NO}_3}$  observed in rivers and surface ocean has mostly been explained by the kinetic isotope fractionation associated with the removal processes such as uptake by phytoplankton and denitrification (Wankel et al. 2006; Ruehl et al. 2007). However, the kinetic isotope fractionation also affects the nitrogen atom of  $\text{NO}_3^-$  and increases the  $\delta^{15}\text{N}_{\text{NO}_3}$  to an extent similar to or even greater than the  $\delta^{18}\text{O}_{\text{NO}_3}$ . Therefore, this mechanism fails to explain the case of the Khura and Trang River estuaries where the  $\delta^{18}\text{O}_{\text{NO}_3}$  alone increased. Wankel et al. (2007) reported a much greater increase in  $\delta^{18}\text{O}_{\text{NO}_3}$  than  $\delta^{15}\text{N}_{\text{NO}_3}$  in several depth profiles obtained in Monterey Bay, California, which is an apparently similar example to the present study. They suggested that the observed ‘decoupling’ of  $\delta^{18}\text{O}_{\text{NO}_3}$  and  $\delta^{15}\text{N}_{\text{NO}_3}$  might be explained by assuming nitrification in the euphotic zone and subsequent partial utilization of this new  $\text{NO}_3^-$  by phytoplankton. The observed variations of  $\delta^{15}\text{N}_{\text{NO}_3}$  and  $\delta^{18}\text{O}_{\text{NO}_3}$  may be partially explained by this model, because both the nitrification and the assimilation apparently contributed to the DIN turnover in these estuaries as discussed earlier. On the other hand, Casciotti et al. (2007) showed that the  $\delta^{18}\text{O}$  of nitrite ( $\text{NO}_2^-$ ) produced by the biochemical reduction of  $\text{NO}_3^-$  could be much higher than original  $\text{NO}_3^-$  due to the branching isotope effect of as large as 25–30‰. If  $\text{NO}_2^-$  thus produced is subsequently reoxidized back to  $\text{NO}_3^-$  keeping the isotopically heavier O atoms, the  $\delta^{18}\text{O}_{\text{NO}_3}$  will increase rapidly with the  $\delta^{15}\text{N}_{\text{NO}_3}$  varying little as the oxidation–reduction cycling

proceeds. This is another possible mechanism that could explain the observed increase of  $\delta^{18}\text{O}_{\text{NO}_3}$  in estuarine waters. However, even if these mechanisms actually caused the observed variations of  $\delta^{15}\text{N}_{\text{NO}_3}$  and  $\delta^{18}\text{O}_{\text{NO}_3}$ , it is still unresolved why they operated exclusively in the polyhaline section in the case of the Khura and Trang Rivers. Tidal water exchange between the mangroves and the estuary proper and some redox processes specific to the sediment/water interface within the mangroves may play an essential role in such phenomena that are apparently confined to the polyhaline section.

Another possible explanation for the steep increase of  $\delta^{18}\text{O}_{\text{NO}_3}$  is the atmospheric deposition of  $\text{NO}_3^-$ , which typically exhibits very high  $\delta^{18}\text{O}$  ( $\geq +60\text{‰}$ ) and various  $\delta^{15}\text{N}$  (Kendall et al. 2007). Estuarine mangrove forests may function as an effective collector and transporter of the atmospheric  $\text{NO}_3^-$  to the estuary. In fact, leaves of the mangrove plant *Rhizophora* spp. along the Khura and Trang Rivers contained water-extractable  $\text{NO}_3^-$  at 20–1,400 nmol per leaf with  $\delta^{15}\text{N}$  and  $\delta^{18}\text{O}$  ranging  $-1$  to  $+6\text{‰}$  and  $+68$  to  $+76\text{‰}$ , respectively (T. Miyajima et al., unpublished data, Feb. 2009). The accumulated  $\text{NO}_3^-$  on the leaf surface can be eventually transferred to the swamp water by litter fall and then transported to the estuary by tidal exchange. Although the final concentration of such  $\text{NO}_3^-$  in the estuarine water should be small compared to the bulk  $\text{NO}_3^-$ , it may raise the  $\delta^{18}\text{O}$  of the estuarine  $\text{NO}_3^-$  to a detectable degree as its  $\delta^{18}\text{O}$  is extremely high.

In summary, this study showed that the river system is not a simple set of channels that gathers terrestrial nitrogen and passes it directly to the coastal ocean, but should be viewed as a series of filters that transform terrestrial nitrogen between organic and inorganic forms and between particulate, dissolved and gaseous forms and consequently moderate the nitrogen flux to the sea. The roles that the river plays in biogeochemical turnover of nitrogen are different between different sections of the river from the upstream freshwater reach to the estuary. In the freshwater reach, the DIN turnover seemed to be nearly in the steady state in the sense that DIN was provided by both external and internal sources and removed principally by internal processes at similar rates. Both the F/B transition zone and the saline-water section could be classified as heterotrophic

systems in view of the carbon and oxygen dynamics. However, the present study suggested that these two sections are not purely heterotrophic (regenerative) in terms of the nitrogen dynamics. Regeneration of DIN seemed to be tightly coupled with the reverse process (immobilization) in the F/B transition zone, and the immobilization and redox cycling of DIN might even prevail over regeneration in the saline-water section. To maintain and take advantage of intrinsic functions of the river in moderating the nitrogen flux to tropical coastal ecosystems, it is indispensable to pay attention to whole biogeochemical functions and maintain the integrity of these biogeochemically active sections of the river system.

**Acknowledgments** This study was supported by the CREST (Core Research for Evolutional Science and Technology) program of Japan Science and Technology Agency, and Grant-in-Aid for Oversea Scientific Research (B) No.16405007 and Grant-in-Aid for Scientific Research (C) No.17510004 from Japan Society for the Promotion of Science. Ranong Coastal Resource Research Station of Kasetsart University and Had-Chao-Mai National Park Education Center kindly provided us with laboratory facilities. The authors gratefully acknowledge M. Nakaoka, C. Aryuthaka, Y. Monthum and T. Srisombat for management of field survey, and S. Pleum-arom, C. Jantharakhantee, T. Niyomsilpchai and N. Thongsin for assistance of field works. The authors were also benefitted by helpful discussion with K. Koba, N. Ohte, N. Ohkouchi, H. Ogawa and M. Tsutsumi on the results and implications of this study, and constructive comments by two anonymous reviewers for the earlier versions of the manuscript.

## References

- Bedard-Haughn A, van Groenigen JW, van Kassel C (2003) Tracing  $^{15}\text{N}$  through landscapes: potential uses and precautions. *J Hydrol (Amst)* 272:175–190. doi:[10.1016/S0022-1694\(02\)00263-9](https://doi.org/10.1016/S0022-1694(02)00263-9)
- Bell PRF (1992) Eutrophication and coral reefs—some examples in the great barrier reef lagoon. *Water Res* 26:553–568. doi:[10.1016/0043-1354\(92\)90228-V](https://doi.org/10.1016/0043-1354(92)90228-V)
- Bernhardt ES, Likens GE, Buso DC, Driscoll CT (2003) In-stream uptake dampens effects of major forest disturbance on watershed nitrogen export. *Proc Natl Acad Sci USA* 100:10304–10308. doi:[10.1073/pnas.1233676100](https://doi.org/10.1073/pnas.1233676100)
- Böhlke JK, Mroczkowski SJ, Coplen TB (2003) Oxygen isotopes in nitrate: new reference materials for  $^{18}\text{O}$ : $^{17}\text{O}$ : $^{16}\text{O}$  measurements and observations on nitrate-water equilibrium. *Rapid Commun Mass Spectrom* 17:1835–1846. doi:[10.1002/rcm.1123](https://doi.org/10.1002/rcm.1123)
- Bouillon S, Connolly RM, Lee SY (2008) Organic matter exchange and cycling in mangrove ecosystems: recent insights from stable isotope studies. *J Sea Res* 59:44–58. doi:[10.1016/j.seares.2007.05.001](https://doi.org/10.1016/j.seares.2007.05.001)
- Brodie J, Fabricius K, De'ath G, Okaji K (2005) Are increased nutrient inputs responsible for more outbreaks of crown-of-thorns starfish? An appraisal of the evidence. *Mar Pollut Bull* 51:266–278. doi:[10.1016/j.marpolbul.2004.10.035](https://doi.org/10.1016/j.marpolbul.2004.10.035)
- Cai W-J, Wiebe WJ, Wang Y, Sheldon JE (2000) Intertidal marsh as a source of dissolved inorganic carbon and sink of nitrate in the Satilla river-estuarine complex in the southeastern U.S. *Limnol Oceanogr* 45:1743–1752
- Cai W-J, Wang Z-A, Wang Y (2003) The role of marsh-dominated heterotrophic continental margins in transport of  $\text{CO}_2$  between the atmosphere, the land-sea interface and the ocean. *Geophys Res Lett* 30:1849. doi:[10.1029/2003GL017633](https://doi.org/10.1029/2003GL017633)
- Casciotti KL, Sigman DM, Hastings MG, Böhlke JK, Hilkert A (2002) Measurement of the oxygen isotopic composition of nitrate in seawater and freshwater using the denitrifier method. *Anal Chem* 74:4905–4912. doi:[10.1021/ac020113w](https://doi.org/10.1021/ac020113w)
- Casciotti KL, Sigman DM, Ward BB (2003) Linking diversity and stable isotope fractionation in ammonia-oxidizing bacteria. *Geomicrobiol J* 20:335–353. doi:[10.1080/014904503003895](https://doi.org/10.1080/014904503003895)
- Casciotti KL, Böhlke JK, McIlvin MR, Mroczkowski SJ, Hannon JE (2007) Oxygen isotopes in nitrite: analysis, calibration, and equilibration. *Anal Chem* 79:2427–2436. doi:[10.1021/ac061598h](https://doi.org/10.1021/ac061598h)
- Clark ID, Fritz P (1997) Environmental isotopes in hydrogeology. Lewis, Boca Raton
- Das A, Krishnaswami S, Bhattacharya SK (2005) Carbon isotope ratio of dissolved inorganic carbon (DIC) in rivers draining the Deccan Traps, India: sources of DIC and their magnitudes. *Earth Planet Sci Lett* 236:419–429. doi:[10.1016/j.epsl.2005.05.009](https://doi.org/10.1016/j.epsl.2005.05.009)
- Diaz RJ, Rosenberg R (2008) Spreading dead zones and consequences for marine ecosystems. *Science* 321:926–929. doi:[10.1126/science.1156401](https://doi.org/10.1126/science.1156401)
- Dijkstra P, LaViolette CM, Coyle JS, Doucet RR, Schwartz E, Hart SC, Hungate BA (2008)  $^{15}\text{N}$  enrichment as an integrator of the effects of C and N on microbial metabolism and ecosystem function. *Ecol Lett* 11:389–397. doi:[10.1111/j.1461-0248.2008.01154.x](https://doi.org/10.1111/j.1461-0248.2008.01154.x)
- Ensign SA, Doyle MW (2006) Nutrient spiraling in streams and river networks. *J Geophys Res* 111:G04009. doi:[10.1029/2005JG000114](https://doi.org/10.1029/2005JG000114)
- Fenton GE, Ritz DA (1988) Changes in carbon and hydrogen stable isotope ratios of macroalgae and seagrass during decomposition. *Estuar Coast Shelf Sci* 26:429–436. doi:[10.1016/0272-7714\(88\)90023-6](https://doi.org/10.1016/0272-7714(88)90023-6)
- Finlay JC, Kendall C (2007) Stable isotope tracing of temporal and spatial variability in organic matter sources to freshwater ecosystems. In: Michener R, Lajtha K (eds) Stable isotopes in ecology and environmental science. Blackwell, Malden, pp 283–333
- Fisher SG, Sponseller RA, Heffernan JB (2004) Horizons in stream biogeochemistry: flowpaths to progress. *Ecology* 85:2369–2379. doi:[10.1890/03-0244](https://doi.org/10.1890/03-0244)
- Frankignoulle M, Abril G, Borges AV, Bourge I, Canon C, Delille B, Libert E, Théate J-M (1998) Carbon dioxide emission from European estuaries. *Science* 282:434–436. doi:[10.1126/science.282.5388.434](https://doi.org/10.1126/science.282.5388.434)

- Granger J, Sigman DM, Needoba JA, Harrison PJ (2004) Coupled nitrogen and oxygen isotope fractionation of nitrate during assimilation by cultures of marine phytoplankton. *Limnol Oceanogr* 49:1763–1773
- Granger J, Sigman DM, Prokopenko MG, Lehmann MF, Tortell PD (2006) A method for nitrite removal in nitrate N and O isotope analyses. *Limnol Oceanogr Methods* 4:205–212
- Grimaldi C, Chaplot V (2000) Nitrate depletion during within-stream transport: effects of exchange processes between stream water, the hyporheic and riparian zones. *Water Air Soil Pollut* 124:95–112. doi:[10.1023/A:1005222513626](https://doi.org/10.1023/A:1005222513626)
- Holmer M (2003) Mangroves of Southeast Asia. In: Black KD, Shimmield GB (eds) *Biogeochemistry of marine systems*. Blackwell, Oxford, pp 1–39
- Jennerjahn TC, Ittekkot V, Klöpper S, Adi S, Nugroho SP, Sudiana N, Yusmal A, Prihartanto, Gaye-Haake B (2004) Biogeochemistry of a tropical river affected by human activities in its catchment: Brantas river estuary and coastal waters of Madura Strait, Java, Indonesia. *Estuar Coast Shelf Sci* 60:503–514. doi:[10.1016/j.ecss.2004.02.008](https://doi.org/10.1016/j.ecss.2004.02.008)
- Kendall C, Mast MA, Rice KC (1995) Tracing watershed weathering reactions with  $\delta^{13}\text{C}$ . In: Kharaka YK, Chudakov OV (eds) *Water-rock interaction*. Balkema, Rotterdam, pp 569–572
- Kendall C, Elliott EM, Wankel SD (2007) Tracing anthropogenic inputs of nitrogen to ecosystems. In: Michener R, Lajtha K (eds) *Stable isotopes in ecology and environmental science*. Blackwell, Malden, pp 375–449
- Kool DM, Wrage N, Oenema O, Dolfing J, Van Groenigen JW (2007) Oxygen exchange between (de)nitrification intermediates and  $\text{H}_2\text{O}$  and its implications for source determination of  $\text{NO}_3^-$  and  $\text{N}_2\text{O}$ : a review. *Rapid Commun Mass Spectrom* 21:3569–3578. doi:[10.1002/rcm.3249](https://doi.org/10.1002/rcm.3249)
- Lapointe BE, Clark MW (1992) Nutrient inputs from the watershed and coastal eutrophication in the Florida Keys. *Estuaries* 15:465–476. doi:[10.2307/1352391](https://doi.org/10.2307/1352391)
- Lapointe BE, Barile PJ, Matzie WR (2004) Anthropogenic nutrient enrichment of seagrass and coral reef communities in the lower Florida Keys: discrimination of local versus regional nitrogen sources. *J Exp Mar Biol Ecol* 308:23–58. doi:[10.1016/j.jembe.2004.01.019](https://doi.org/10.1016/j.jembe.2004.01.019)
- Lehmann MF, Bernasconi SM, Barbieri A, McKenzie JA (2002) Preservation of organic matter and alteration of its carbon and nitrogen isotope composition during simulated and in situ early sedimentary diagenesis. *Geochim Cosmochim Acta* 66:3573–3584. doi:[10.1016/S0016-7037\(02\)00968-7](https://doi.org/10.1016/S0016-7037(02)00968-7)
- Lehmann MF, Reichert P, Bernasconi SM, Barbieri A, McKenzie JA (2003) Modelling nitrogen and oxygen isotope fractionation during denitrification in a lacustrine redox-transition zone. *Geochim Cosmochim Acta* 67:2529–2542. doi:[10.1016/S0016-7037\(03\)00085-1](https://doi.org/10.1016/S0016-7037(03)00085-1)
- Mariotti A, Germon JC, Hubert P, Kaiser P, Letolle R, Tardieu A, Tardieu P (1981) Experimental determination of nitrogen kinetic isotope fractionation: some principle; illustration for the denitrification and nitrification processes. *Plant Soil* 62:413–430. doi:[10.1007/BF02374138](https://doi.org/10.1007/BF02374138)
- McClelland JW, Valiela I (1998) Linking nitrogen in estuarine producers to land-derived sources. *Limnol Oceanogr* 43:577–585
- McCook LJ, Jompa J, Diaz-Pulido G (2001) Competition between corals and algae on coral reefs: a review of evidence and mechanisms. *Coral Reefs* 19:400–417. doi:[10.1007/s003380000129](https://doi.org/10.1007/s003380000129)
- Millero FJ, Graham TB, Huang F, Bustos-Serrano H, Pierrot D (2006) Dissociation constants of carbonic acid in seawater as a function of salinity and temperature. *Mar Chem* 100:80–94. doi:[10.1016/j.marchem.2005.12.001](https://doi.org/10.1016/j.marchem.2005.12.001)
- Miyajima T, Yamada Y, Hanba YT, Yoshii K, Koitabashi T, Wada E (1995) Determining the stable isotope ratio of total dissolved inorganic carbon in lake water by GC/C/IRMS. *Limnol Oceanogr* 40:994–1000
- Miyajima T, Tsuboi Y, Tanaka Y, Koike I (2009) Export of inorganic carbon from two Southeast Asian mangrove forests to adjacent estuaries as estimated by the stable isotope composition of dissolved inorganic carbon. *J Geophys Res* 114:G01024. doi:[10.1029/2008JG000861](https://doi.org/10.1029/2008JG000861)
- Montoya JP, McCarthy JJ (1995) Isotopic fractionation during nitrate uptake by phytoplankton grown in continuous culture. *J Plankton Res* 17:439–464. doi:[10.1093/plankt/17.3.439](https://doi.org/10.1093/plankt/17.3.439)
- Mulholland PJ (1992) Regulation of nutrient concentrations in a temperate forest stream: roles of upland, riparian, and instream processes. *Limnol Oceanogr* 37:1512–1526
- Needoba JA, Waser NA, Harrison PJ, Calvert SE (2003) Nitrogen isotope fractionation in 12 species of marine phytoplankton during growth on nitrate. *Mar Ecol Prog Ser* 255:81–91. doi:[10.3354/meps255081](https://doi.org/10.3354/meps255081)
- Neubauer SC, Anderson IC (2003) Transport of dissolved inorganic carbon from a tidal freshwater marsh to the York river estuary. *Limnol Oceanogr* 48:299–307
- Pawellek F, Veizer J (1994) Carbon cycle in the upper Danube and its tributaries:  $\delta^{13}\text{C}$ -DIC constraints. *Isr J Earth Sci* 43:187–194
- Ruehl CR, Fisher AT, Huertos ML, Wankel SD, Wheat CG, Kendall C, Hatch CE, Shennan C (2007) Nitrate dynamics within the Pajaro river, a nutrient-rich, losing stream. *J N Am Benthol Soc* 26:191–206. doi:[10.1899/0887-3593\(2007\)26\[191:NDWTPRJ\]2.0.CO;2](https://doi.org/10.1899/0887-3593(2007)26[191:NDWTPRJ]2.0.CO;2)
- Sato T, Miyajima T, Ogawa H, Umezawa Y, Koike I (2006) Temporal variability of stable carbon and nitrogen isotopic composition of size-fractionated particulate organic matter in the hypertrophic Sumida river estuary of Tokyo Bay, Japan. *Estuar Coast Shelf Sci* 68:245–258. doi:[10.1016/j.ecss.2006.02.007](https://doi.org/10.1016/j.ecss.2006.02.007)
- Sebilo M, Billen G, Grably M, Mariotti A (2003) Isotopic composition of nitrate-nitrogen as a marker of riparian and benthic denitrification at the scale of the whole Seine River system. *Biogeochemistry* 63:35–51. doi:[10.1023/A:1023362923881](https://doi.org/10.1023/A:1023362923881)
- Sebilo M, Billen G, Mayer B, Billiou D, Grably M, Garnier J, Mariotti A (2006) Assessing nitrification and denitrification in the Seine river and estuary using chemical and isotopic techniques. *Ecosystems* (N Y, Print) 9:564–577. doi:[10.1007/s10021-006-0151-9](https://doi.org/10.1007/s10021-006-0151-9)
- Seitzinger SP, Kroeze C (1998) Global distribution of nitrous oxide production and N inputs in freshwater and coastal marine ecosystems. *Glob Biogeochem Cycles* 12:93–113. doi:[10.1029/97GB03657](https://doi.org/10.1029/97GB03657)
- Sigman DM, Casciotti KL, Andreani M, Barford C, Galanter M, Böhlke JK (2001) A bacterial method for the nitrogen

- isotopic analysis of nitrate in seawater and freshwater. *Anal Chem* 73:4145–4153. doi:[10.1021/ac010088e](https://doi.org/10.1021/ac010088e)
- Sigman DM, Robinson R, Knapp AN, van Geen A, McCorkle DC, Brandes JA, Thunell RC (2003) Distinguishing between water column and sedimentary denitrification in the Santa Barbara Basin using the stable isotopes of nitrate. *Geochem Geophys Geosyst* 4:1040. doi:[10.1029/2002GC000384](https://doi.org/10.1029/2002GC000384)
- Sigman DM, Granger J, DiFiore PJ, Lehmann MM, Ho R, Cane G, van Geen A (2005) Coupled nitrogen and oxygen isotope measurements of nitrate along the eastern North Pacific margin. *Glob Biogeochem Cycles* 19:GB4022. doi:[10.1029/2005GB002458](https://doi.org/10.1029/2005GB002458)
- Sugimoto R, Kasai A, Miyajima T, Fujita K (2008) Nitrogen isotopic discrimination by water column nitrification in a shallow coastal environment. *J Oceanogr* 64:39–48. doi:[10.1007/s10872-008-0003-7](https://doi.org/10.1007/s10872-008-0003-7)
- Trudeau V, Rasmussen JB (2003) The effect of water velocity on stable carbon and nitrogen isotope signatures of periphyton. *Limnol Oceanogr* 48:2194–2199
- Umezawa Y, Hosono T, Onodera S, Siringan F, Buapeng S, Delinom R, Yoshimizu C, Tayasu I, Nagata T, Taniguchi M (2008) Sources of nitrate and ammonium contamination in groundwater under developing Asian megacities. *Sci Total Environ* 404:361–376. doi:[10.1016/j.scitotenv.2008.04.021](https://doi.org/10.1016/j.scitotenv.2008.04.021)
- Vörösmarty CJ, Fekete BM, Tucker BA (1996) Global river discharge database (RivDIS v1.0) II. Asia. University of New Hampshire, Durham
- Wankel SD, Kendall C, Francis CA, Paytan A (2006) Nitrogen sources and cycling in the San Francisco bay Estuary: a nitrate dual isotopic composition approach. *Limnol Oceanogr* 51:1654–1664
- Wankel SD, Kendall C, Pennington JT, Chavez FP, Paytan A (2007) Nitrification in the euphotic zone as evidenced by nitrate dual isotopic composition: observations from Monterey Bay, California. *Glob Biogeochem Cycles* 21:GB2009. doi:[10.1029/2006GB002723](https://doi.org/10.1029/2006GB002723)
- Weiss RF (1974) Carbon dioxide in water and seawater: the solubility of non-ideal gas. *Mar Chem* 2:203–215. doi:[10.1016/0304-4203\(74\)90015-2](https://doi.org/10.1016/0304-4203(74)90015-2)